ELSEVIER

Journal of Structural Geology 29 (2007) 18–35

JOURNAL OF STRUCTURAL GEOLOGY

www.elsevier.com/locate/jsg

Progressive deformation partitioning and deformation history: Evidence from millipede structures

T.H. Bell*, M.D. Bruce

School of Earth Sciences, James Cook University, Townsville, Qld 4811, Australia

Received 23 March 2006; received in revised form 15 August 2006; accepted 16 August 2006
Available online 25 October 2006

Abstract

The progressive development and migration of patterns of deformation partitioning at all scales through the rock matrix commonly destroys any record of the ductile history associated with previous events making the problem of similar structures developing through multiple pathways generally intractable. However, records of the small-scale geometries that form as deformation commences and begins to partition through a rock are routinely trapped and protected by porphyroblasts because these large crystals nucleate and/or grow at this time. This allows examination of the geometry of microstructures formed at the start of deformation partitioning that were destroyed by the same event in the matrix, or which formed during an event prior to any preserved in the matrix. Porphyroblasts locally preserve oppositely concave microfolds (''millipedes''), which, in all examples that we have found, exclusively indicate a deformation history of bulk inhomogeneous shortening. Very similar structures have been formed experimentally during inhomogeneous simple shear but can readily be distinguished from those trapped in porphyroblasts that form during progressive bulk inhomogeneous shortening. Oppositely concave microfolds in some porphyroblasts reveal that deformation near orthogonal to a previously developed foliation occurred by axial plane shear driven rotation that led to rapid reactivational ''card-deck-like'' collapse of the pre-existing foliation. Differentiated crenulation cleavages may result from the same process providing yet another reason for the cessation of porphyroblast growth at the start of differentiation.

Keywords: Progressive bulk inhomogeneous shortening; Shear sense; Porphyroblast nucleation; Porphyroblast growth; Coaxial deformation; Crenulation cleavage development

1. Introduction

Deformation partitioning (illustrated in Fig. 1) plays a significant role in numerous processes that accompany tectonism (Siame et al., 2005). These include the development of foliations of all types other than bedding (Bell, 1981; Davis, 1995), porphyroblast nucleation and growth within a sample (Hayward, 1992), sites of recrystallization during mylonitization (Bell and Johnson, 1989), dissolution and solution transfer (Stewart, 1997), crystal-plasticity versus solution-transfer (Lagoeiro et al., 2003), the leaching and transport of metals from low concentration environments to ones where orebodies develop (Davis, 2004), the development of meso and microstructures used for shear sense determinations (Bell and Johnson, 1992), and sites for the formation of metamorphogenic ore bodies (Aerden, 1991). The effects of deformation partitioning are obvious in the case of localization of shearing on the boundary of more competent rocks such as a granite pluton, where the rheological contrasts between the intrusion and the country rocks provide a ready explanation for the geometry observed. However, the effects and role of deformation partitioning are much less certain in the development of crenulation cleavages in massive slates and schists or anastomosing shear zones in granitoids and amphibolites, where the rock was more homogeneous to start with. Little is known about the progressive development of this phenomenon in tectonized rocks because the distribution of zones of progressive shearing and shortening (that is the pattern of partitioning;

* Corresponding author. Tel.: +61 7 4781 4766; fax: +61 7 4725 1501.
E-mail address: tim.bell@jcu.edu.au (T.H. Bell).

0191-8141/$ - see front matter © 2006 Elsevier Ltd. All rights reserved.
doi:10.1016/j.jsg.2006.08.005

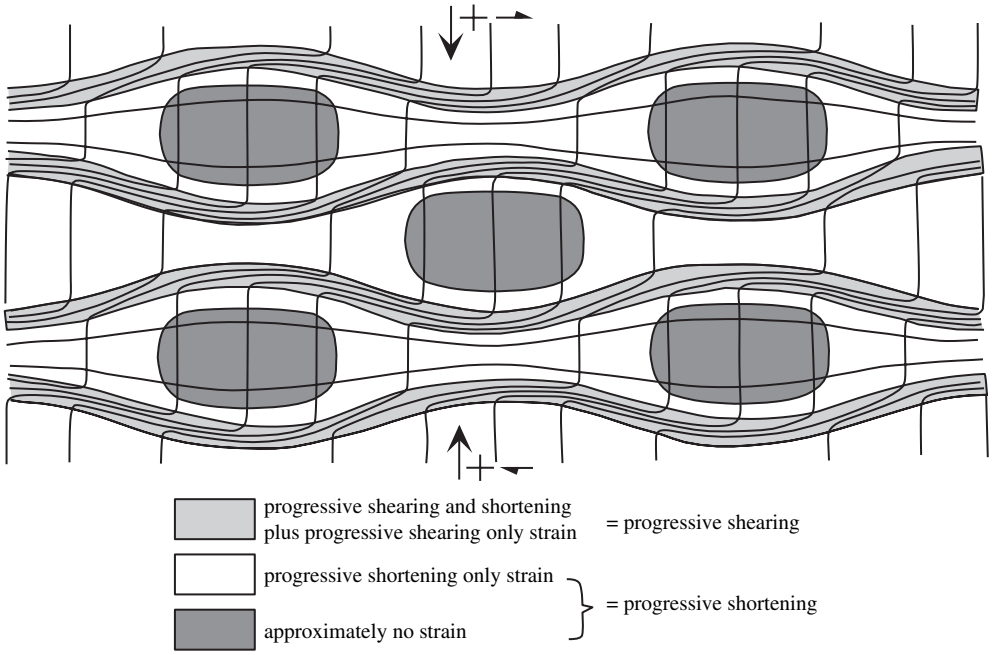

Fig. 1. Shows the partitioning of deformation into zones of no strain, progressive shortening strain, progressive shearing plus shortening strain, and progressive shearing only strain that results from a history of deformation involving progressive bulk inhomogeneous shortening (thick arrows) with a component of anticlockwise shear (thin single barbed arrows; after Bell, 1981). For discussion we group the zones of no strain and progressive shortening only strain and call them progressive shortening. We group the zones of progressive shortening plus shearing and progressive shearing strain and call them zones of progressive shearing.

e.g., Figs. 1 and 2a,b) changes as the deformation proceeds and early stages are obliterated by the overprinting effects of later stages in the same event, as well as by subsequent events.

Quantitative structural studies of porphyroblasts involving the routine measurement of inclusion trail geometries, have provided substantial evidence that these large crystals preserve considerable data on the history of the progressive role of deformation partitioning in the surrounding rocks (e.g., Bell et al., 2004; Cihan and Parsons, 2005; Sayab, 2005). Once the P, T and bulk composition are appropriate, porphyroblasts grow in zones of progressive shortening that result from deformation partitioning at a scale similar to their maximum size and cease growth once a pattern of non-coaxial deformation is established and differentiation begins. For porphyroblasts to nucleate or regrow in these zones, a pre-existing, foliation lying at a high angle to any newly developing one must be

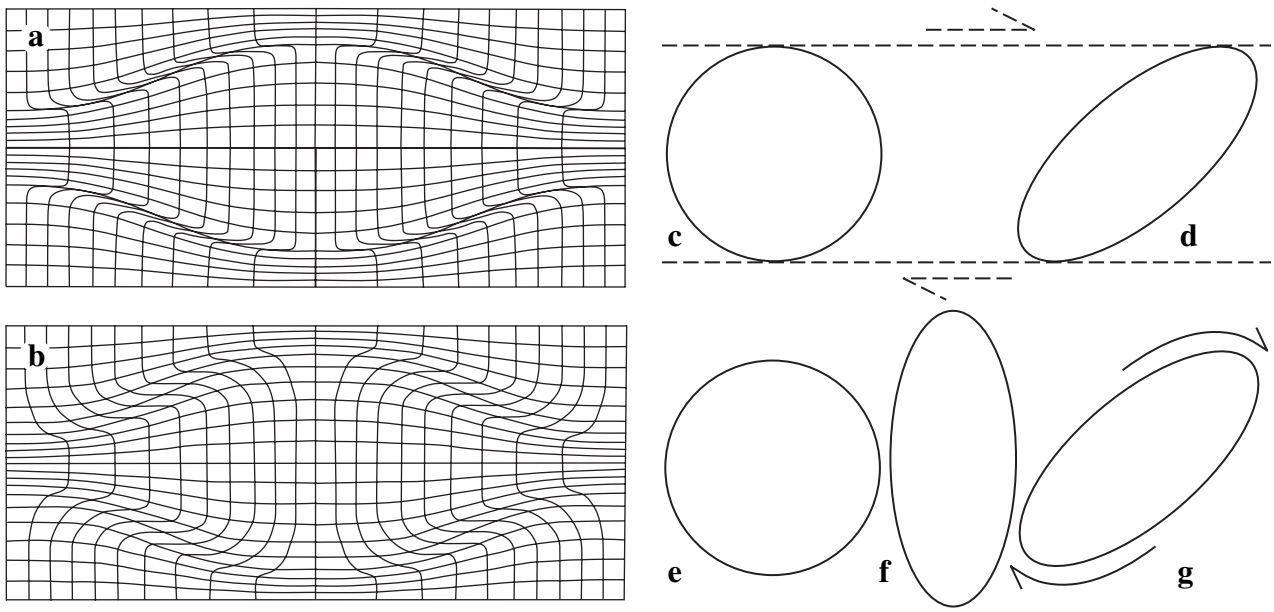

Fig. 2. (a, b) The millipede shaped geometry of the strain field that results from coaxial progressive bulk inhomogeneous shortening. The progressive shearing component of the deformation is more confined in (a) than in (b). (c, d) Schematic representation of the transformation of a sphere (c) by progressive simple shear to an ellipsoid. (e–g) Schematic representation of the transformation of a sphere (e) by progressive homogenous shortening (progressive pure shear; f), plus a rotation (g), to the same end product as in (d).

present and there should be limited or no reactivation of the compositional layering (Bell et al., 2003).

Oppositely concave microfolds preserved in porphyroblasts (millipedes; Figs. 2a,b) potentially provide a geometry that contains unique evidence of the deformation history that a rock has been through (Bell, 1981). Some results from experimental models produced in the seventies appear to suggest that this might not be the case (Ghosh, 1975). We re-examine natural and experimentally derived geometries and conclude that all oppositely concave microfolds that we have examined in rocks provide a unique insight into at least a portion of the deformation history that the host rocks have undergone. This insight leads to revelations on the role of near orthogonal foliations in crenulation cleavage development and the cessation of porphyroblast growth.

2. Deformation history

2.1. The non-uniqueness of most structures

Most structures can be produced through different deformation history paths. In particular, structures that result from some form of inhomogeneous shortening (e.g., Fig. 1) can also be produced by some combination of shearing plus rotation of the whole geometry or through overprinting by shearing in another direction. The simplest example of this is progressive pure shear versus progressive simple shear where the strain geometry produced by simple shear in Figs. 2c,d is produced by pure shear plus a rotation in Figs. 2e–g. Folds preserved in porphyroblasts that are oppositely concave along their axial plane with the transition containing straight layers as shown in Figs. 2a,b (millipede geometry) appeared to be uniquely a product of progressive bulk inhomogeneous shortening. However, Johnson and Bell (1996) suggested that such structures may not be unique because similar ones had been produced experimentally during modelling of progressive simple shear (Ghosh, 1975). This possibility is re-examined below.

2.2. Are millipede geometries a unique indicator of deformation history?

Ghosh (1975) reported experiments in which silicone putty containing rigid wood cylinders was deformed by progressive simple shear (Figs. 3 and 4). He marked each experimental run with a passive marker from which an estimate of the resultant 2-D strain field geometry can be determined. He marked some with indented circles, which on deformation became strain ellipses, allowing an estimate of the foliation generated by the deformation to be determined. His starting configuration in Fig. 3a shows a rigid circular central cylinder, plus lines in grey (the marker) and the circles in light grey that were indented into the silicone putty matrix (which define strain ellipses after deformation has been imposed). The final strain state in Fig. 3b shows the effects of anticlockwise progressive simple shear on rotation of the rigid cylinder, the markers and the indented circles; the latter become ellipses. Significantly,

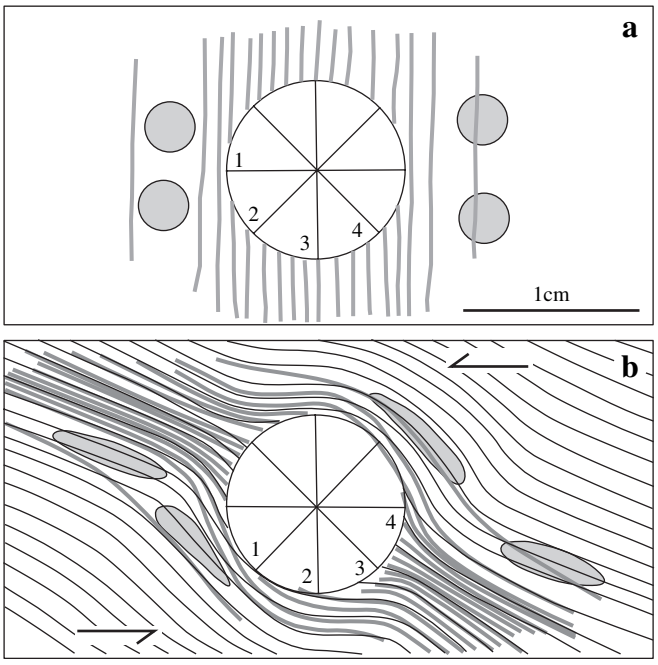

Fig. 3. (a) Accurately reproduced line diagram from Fig. 8 in Ghosh (1975) of rigid cylinder in silicone putty at start of an experimental run involving top to left (anticlockwise) shear. Prior to commencement of the experiment the grey lines were marked and the grey in filled circles were inscribed (as circles) into the model; they become strain markers. (b) Accurately reproduced line diagram from Fig. 10 in Ghosh (1975) at the end of the experimental run involving anticlockwise progressive simple shear. The finer lines are strain lines developed in the silicone putty and were drawn onto the image at very high magnification. They lie parallel to the strain ellipsoids. Single barbed arrows show direction of shear applied to produce this geometry.

heterogeneities that develop in the silicone putty with deformation follow the strain ellipses and can be used to define the ''foliation'' that develops during the experimental deformation. These matrix silicone putty ''foliations'' were drawn on the photo in Fig. 10 from Ghosh (1975) after it had been reproduced at high magnification on a computer. Where the markers lie at a high angle to the newly developing foliation, as shown in Fig. 3, a shear zone-type geometry forms. Where they lie at a moderate angle and dip in the direction of relative shear, a millipede-like geometry can be formed (Fig. 4).

Fig. 4 shows the pre-deformation, intermediate and final states of strain for the same experiment as in Fig. 3 (Figs. 11, 12b and 13 respectively in Ghosh, 1975) but where the markers lay at 45° to the shear plane, oriented so that during anticlockwise progressive shearing they would initially undergo shortening (compare Figs. 4a,b). The ''foliation'' developing as a result of this deformation, which is defined by the matrix silicone putty strain lines that were drawn on the photo at high magnification, is shown in Figs. 4b,c. As described by Johnson and Bell (1996), the grey lines defining the initial ''foliation'' are deformed into millipede-like shapes in Figs. 4b,c. However, when one compares these shapes (Figs. 5a,b) with the newly developed ''foliation'' the difference between this geometry and the natural millipede shown in Fig. 5c is apparent around the porphyroblast margins that lie parallel to the newly developed foliation. In natural millipedes, the newly

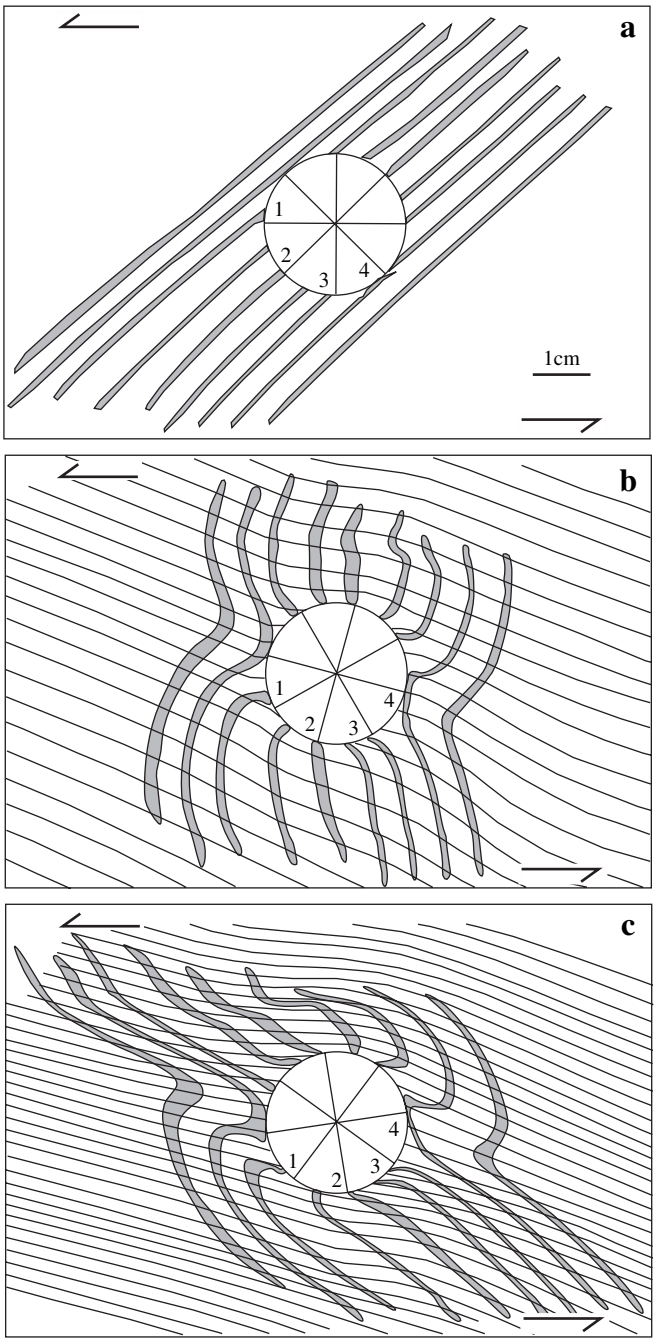

Fig. 4. (a) Accurately reproduced line diagram from Fig. 11 in Ghosh (1975) of rigid cylinder in silicone putty at start of an experimental run involving top to left (anticlockwise) shear (shown by arrows). The grey lines become strain markers. (b) Accurately reproduced line diagram from Fig. 12b in Ghosh (1975) part way through experimental run involving progressive simple shear. The finer lines are strain lines developed in the silicone putty and were drawn onto the image at very high magnification. They lie parallel to the local strain ellipsoid and define a foliation. (c) As for (b) except at higher strain at the end of the experimental run. Single barbed arrows show direction of shear applied to produce these geometries.

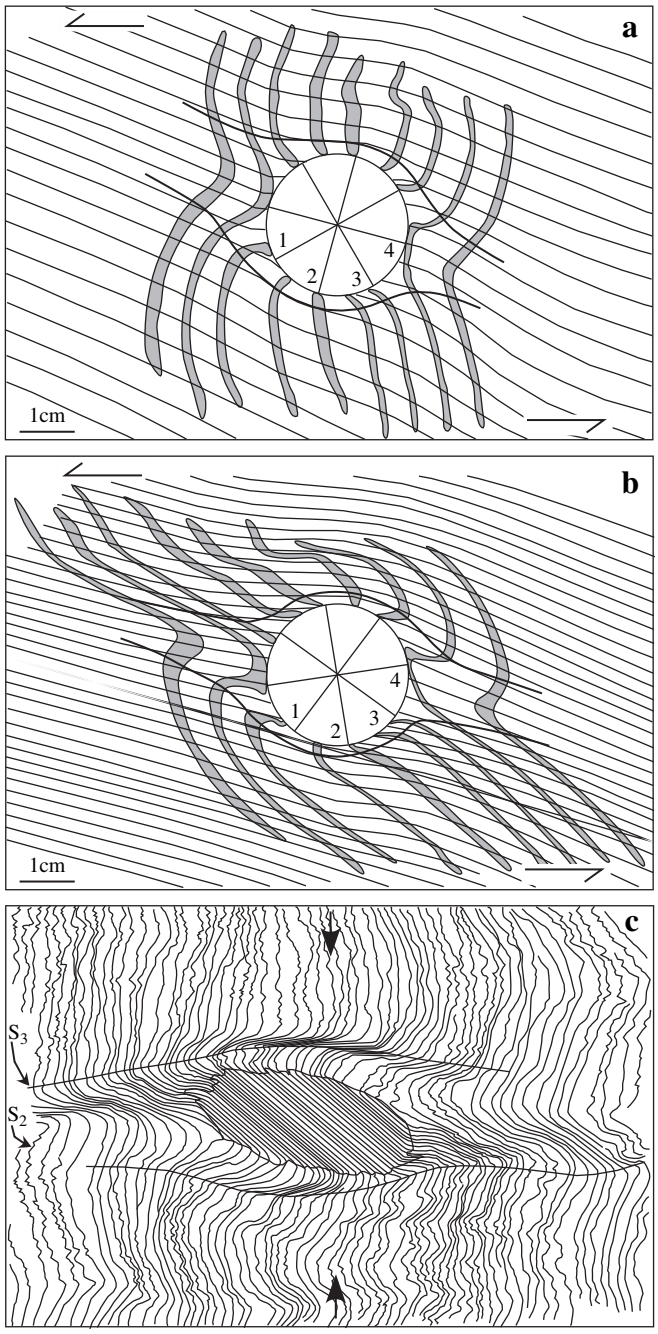

Fig. 5. (a, b) Shows millipede like geometries (oppositely concave folds) produced experimentally by progressive simple shear. The foliation (thin lines) cuts across the millipede fold axial planes to either side of the core structure (thicker lines). Single barbed arrows show direction of shear applied to produce this geometry. (c) Shows a natural millipede geometry within a porphyroblast produced by progressive bulk inhomogeneous shortening. The differentiated crenulation cleavage (foliation) produced during the millipede event follows the axial planes of the folds to either side of the core structure (thick lines). Arrows show the inferred direction of bulk shortening that produced this geometry.

developed foliation follows the hinge line from one direction of curvature to the opposite as seen in Fig. 5c around the porphyroblast rim. For millipede-like shapes formed during a history of progressive simple shear, this is not the case. The foliation that developed during deformation cuts across the axial planes defined by the millipede-like shapes. Beaumont-Smith (2001) suggested that millipede geometries might result from conjugate crenulations forming around a porphyroblast that were then overgrown by the porphyroblast rim. However, his "conjugate" crenulations are simply the anastomosing

crenulation geometries that develop during the early coaxial stages prior to the development of a differentiated crenulation cleavage (Figs. 6a–f) and no different to the geometries that we describe (e.g., Bell et al., 2004).

3. Examples of very coaxial geometries

3.1. Millipede generating fold hinge

Figs. 7 and 8 show a D_3 fold hinge (Sample H20C) from an amphibolite facies outcrop of a muscovite and quartz rich schist containing numerous plagioclase porphyroblasts in the Robertson River metamorphics where the first millipede microstructures were recognized (Bell and Rubenach, 1980). This sample contains 3 foliations that can be readily observed under the microscope. The axial plane structure is a differentiated crenulation cleavage called S_3 (Fig. 9). The folded foliation (Figs. 7–9), which is crenulated microscopically to form S_3 seams (Figs. 9c–e), is also a differentiated crenulation cleavage called S_2 (Fig. 9a). Between the S_2 cleavage seams a crenulated cleavage called S_1 is preserved (Figs. 9a,c and 10a,b). Attempts at modelling the progressive development of the millipede microstructures in this outcrop resulted in the strain field geometry shown in Figs. 1 and 2a,b and the

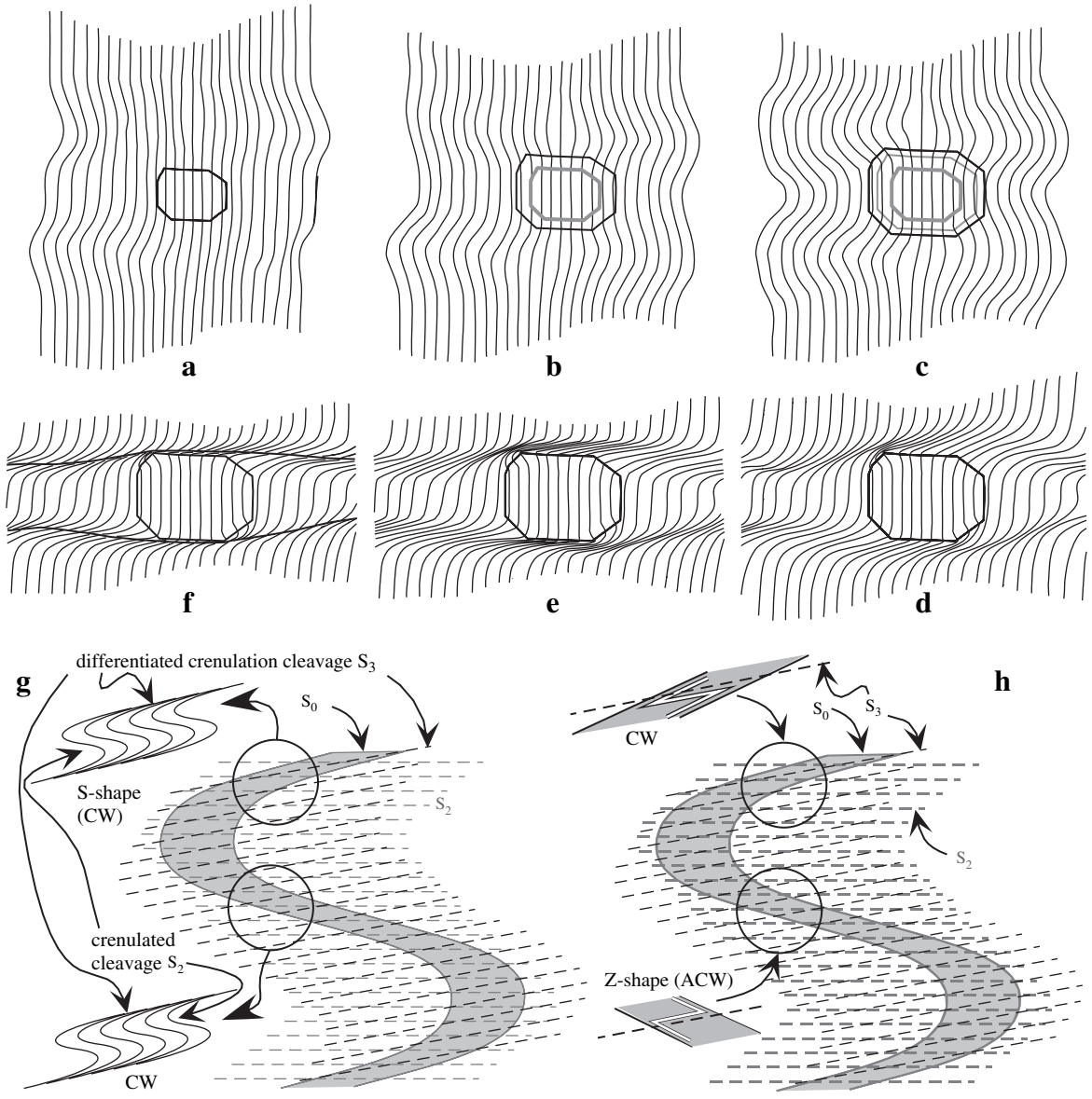

The differentiation asymmetry of S_2 on S_3 does not change across the D_2 fold but the vergence asymmetry of S_0 on S_3 does.

Fig. 6. Shows how porphyroblast growth that has commenced very early during a deformation event (a–c) ceases once a differentiated crenulation cleavage begins to form in the immediate vicinity (d–f). The progression shows how the core may preserve a coaxial millipede geometry (a–c), but the more developed matrix contains a consistent clockwise non-coaxial asymmetry at stages (d–f). This figure also shows how nucleation of a porphyroblastic phase for the first time at a particular site requires partitioning of the deformation into progressive shearing and shortening components, on the scale of a porphyroblast, through that location. The differentiation asymmetry (g), which in this example is the curvature of S_2 into differentiated S_3 (see Bell et al., 2003), is clockwise and does not change across the fold although the vergence asymmetry (h) of S_0 relative to S_3 does. The foliation/foliation asymmetry of S_2 relative to S_3 does not change either.

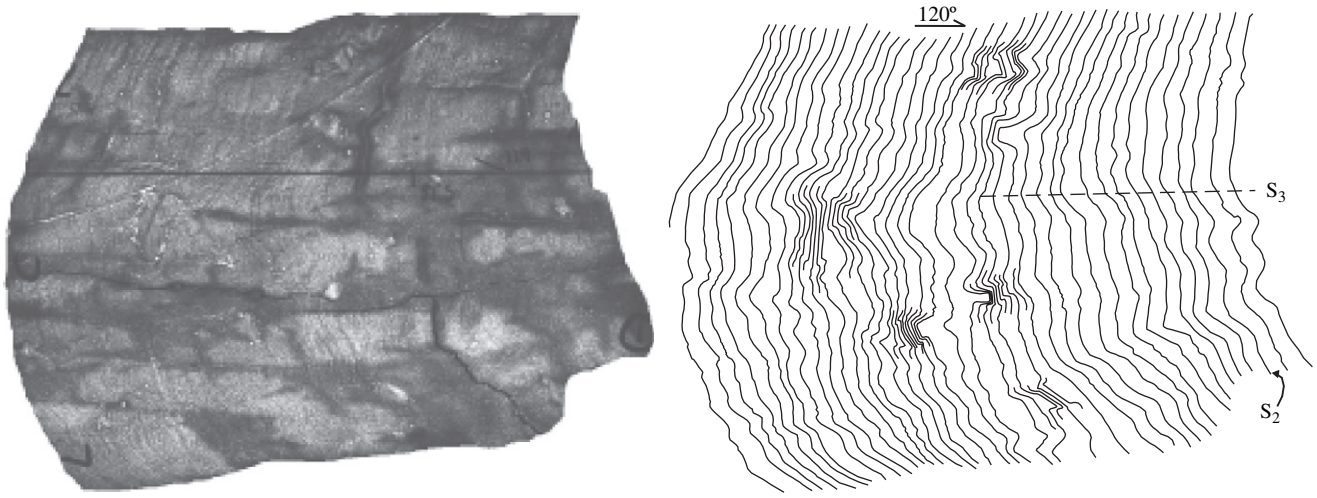

Fig. 7. Fold hinge from outcrop containing numerous plagioclase porphyroblasts all of which examined in thin section contain millipede microstructure. The axial plane structure is readily apparent in thin sections and is called S_3. The folded foliation is called S_2. The differentiation asymmetry of S_2 into S_3 in the matrix on both limbs is predominantly clockwise looking in the direction shown (that is, it looks the same as that shown in Figs. 6d–f on a microscope). The single barbed arrow shows the strike of the sub-vertical profile plane. Width perpendicular to axial plane is 10 cm.

concepts on the role of deformation partitioning in its development that were described by Bell (1981). This fold hinge formed during the same deformation event that developed the millipede microstructures.

The asymmetry of curvature of a crenulated cleavage into an overprinting differentiated crenulation cleavage (Figs. 6d–f), called the differentiation asymmetry (which is clockwise in the matrix in Figs. 6d–f), does not necessarily change across a fold hinge (compare Figs. 2b,d in Bell et al., 2003). In the case of the fold shown in Figs. 7 and 8 the asymmetry of curvature of crenulated S_2 into differentiated crenulation cleavage S_3 remains clockwise on both limbs in the matrix away from porphyroblasts. This differs from the foliation/foliation asymmetry of S_2 relative to S_3 across the fold, which switches from limb to limb (e.g. Bell et al., 2003). This fold contains numerous plagioclase porphyroblasts, all of which preserve superb millipede-shaped quartz inclusion trail geometries with the example shown in Fig. 9 containing the most oblique relationship between S_2 and S_3 that was found. Generally it is only in regions adjacent to these porphyroblasts that local anticlockwise curvature of S_2 into S_3 is preserved. One thin section was cut from each of the lower and upper limbs and the hinge of 4 separate profile plane slabs of this fold as shown in Figs. 8a,b; the profile plane dips 80°S, strikes at 120° and the fold was cylindrical on the scale of the outcrop. Thin sections were also cut from the lower and upper limbs plus hinge in 4 slabs cut parallel to L_3^2 and perpendicular to S_3, as shown in Figs. 8a,c.

All porphyroblasts present in each of the 12 thin sections from the profile plane of the fold (Fig. 8b) contain millipede inclusion trail geometries. The straight foliation defined by the bulk of the inclusion trails across the core of all the porphyroblasts on the lower limb of the fold (the location of the thin section blocks are shown in Fig. 8b) pitches SE. It is

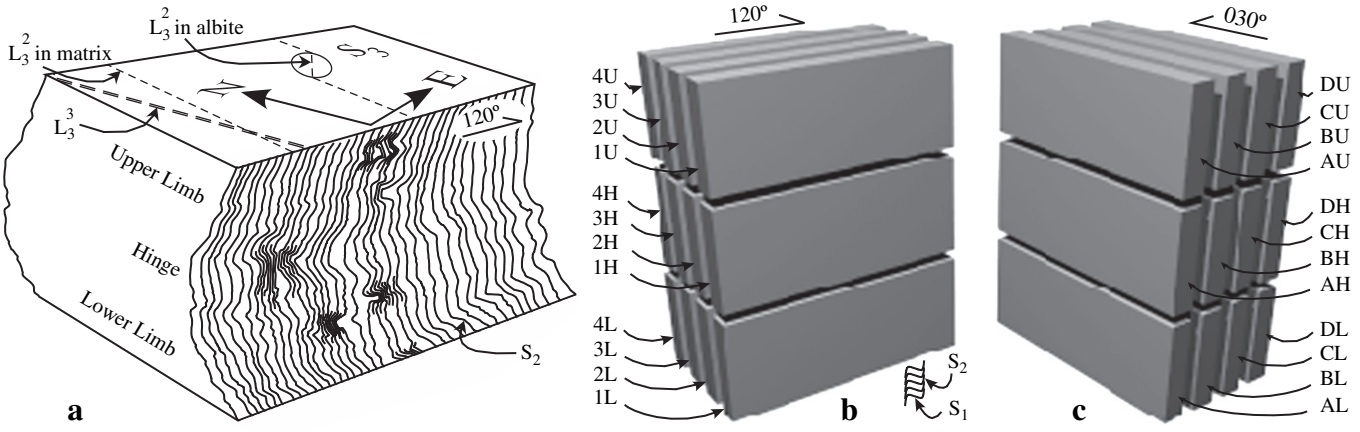

Fig. 8. Fold hinge (a) showing the relative orientation and locations of blocks from which thin sections (b) were cut in the profile plane (width perpendicular to axial plane is 10 cm). (c) Parallel to the F_3^2 fold axis but perpendicular to the S_3 axial plane. The differentiation asymmetry due to the curvature of crenulated S_1 into the differentiated crenulation cleavage S_2 that is folded around the fold is also shown as it appears in the profile plane.

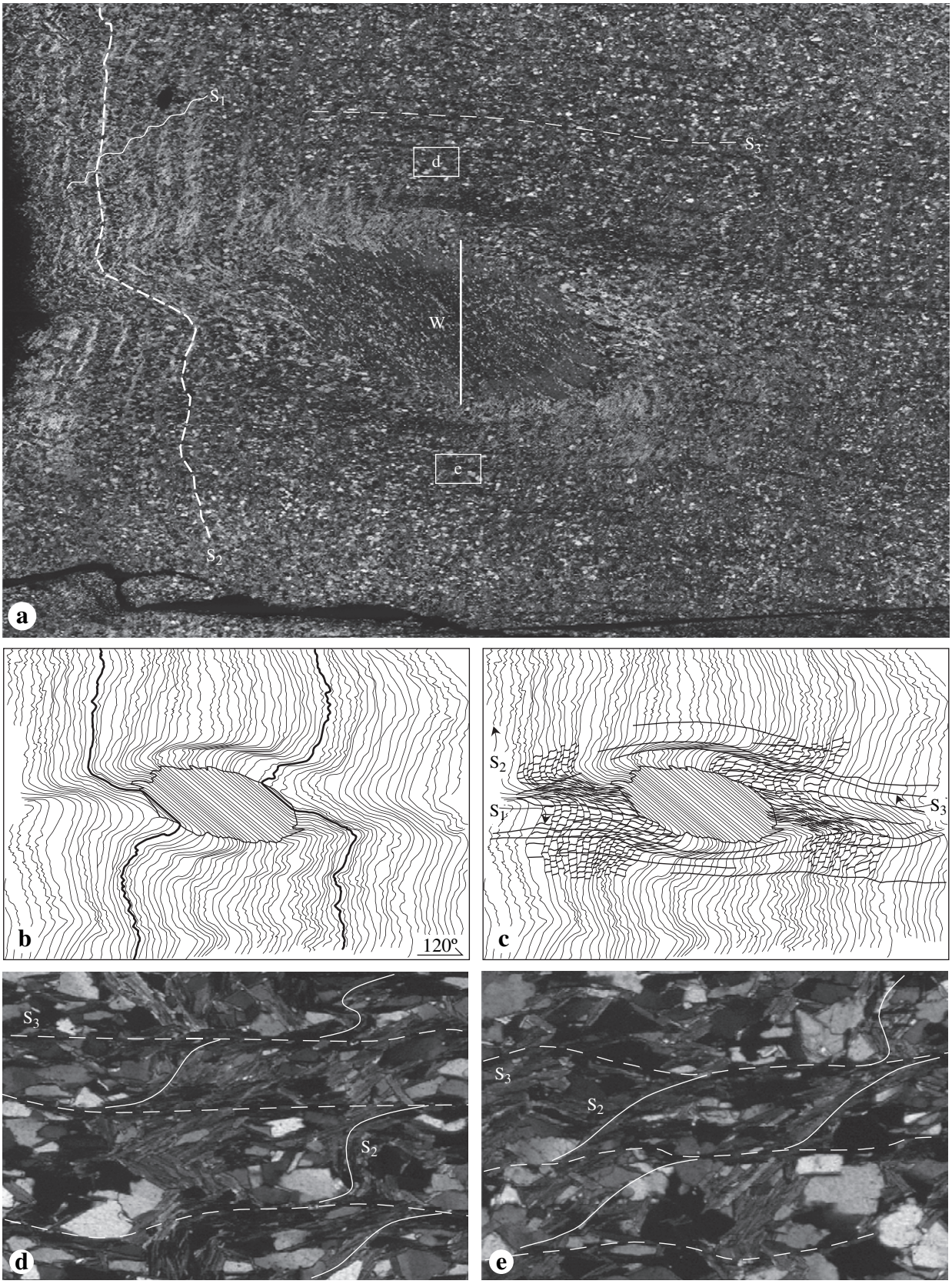

Fig. 9. (a) Plagioclase porphyroblast containing highly oblique millipede-shaped trails from the hinge of the fold in Fig. 7 (vertical width is 2.5 cm). (b) Shows the S_2 foliation, which predates porphyroblast growth, and which was accurately drawn onto the image in (a) at very high magnification. Note the spectacular increase in width parallel to the axial plane S_3 between S_2 planes, from inside to outside the porphyroblast (1.83 times). This is best observed using the two S_2 traces outlined with heavy black lines as they pass out of either end of the porphyroblast and is due the effects of bulk shortening near orthogonal to S_3. (c) Shows changes in crenulated cleavage S_1 as S_2 passes through the porphyroblast strain shadow. Also shows local more intense zones of sub-horizontal differentiated crenulation cleavage S_3 adjacent to the porphyroblast. (d) Detail of boxed area marked d in (a) showing clockwise differentiation asymmetry of S_2 into S_3. (e) Detail of boxed area marked e in (a) showing clockwise differentiation asymmetry of S_2 into S_3.

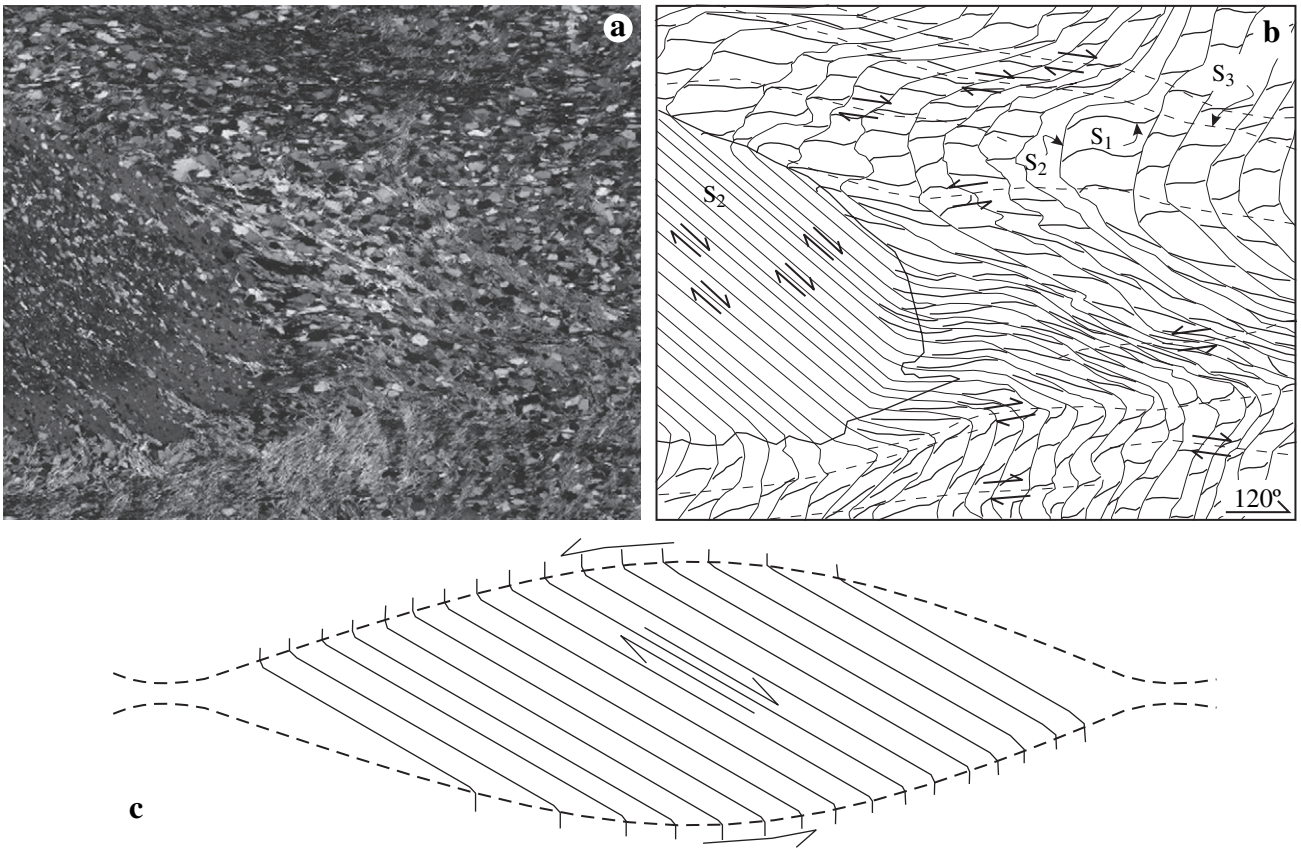

Fig. 10. (a) Photographic detail of right hand millipede end. (b) Shows S_1, S_2 and S_3. Note that S_1 inside and outside the triangular shaped strain shadow on the right side of the porphyroblast does not cut across S_2. Shear on S_3 in the matrix switches from clockwise (3 heavy short arrows above and 3 below) to anticlockwise (2 heavy short arrows to right of albite) on S_3 bounding the strain shadow. The S_1 into S_2 differentiation asymmetry outside the porphyroblast strain shadow is anticlockwise. Inside the strain shadow it is clockwise. This resulted from the clockwise reactivation of S_2 early during D_3 that switched the primary anticlockwise differentiation asymmetry of S_1 into S_2 outside of the porphyroblast strain shadow to clockwise within the strain shadow. (c) Schematically summarizes the clockwise reactivation of S_2 that took place within an ellipsoidal pod of partitioned D_3 strain, which rotated S_2 prior to growth of the porphyroblast. The porphyroblast and its strain shadow fill this pod although modification of the strain shadow occurred as D_3 intensified. This pulled S_2 seams apart and elongated relic S_1 lying between them as can be seen in (b).

significant (see below) that in the hinge and upper limb this foliation locally pitches NE; therefore, this data is distinguished in Table 1, as are the widths of the zones of partitioned strain that contain the porphyroblasts in Table 2. A photo of the porphyroblast in the hinge region that contains inclusion trails pitching at the lowest angle (45°SE) is shown in Fig. 9a (see below).

We measured the width perpendicular to S_3 across the widest part of each porphyroblast (W in Fig. 9a) in the 12 profile plane thin sections mentioned above as well as 12 thin sections cut from 4 vertical slabs (using the thin section blocks shown in Fig. 8c). We did this to provide a measure of the width of the millipede shaped zone of deformation partitioning within which the porphyroblast grew to see if any differences related to the variation in inclusion trail pitch for the lower limb versus the hinge and upper limb were observable (Table 2). Such measurements are completely dependent on where the thin section cuts through each porphyroblast measured. However, sufficient porphyroblasts were found in each limb for the average width obtained to have some significance. The average width of this zone in the lower limb, where all the porphyroblasts contain inclusions dipping towards the SE in 3-D, is 6.00 mm (Table 2). The average width of this zone for porphyroblasts containing inclusion trails that do not have the lower limb dip direction is 2.63 mm in the hinge and 3.73 mm in the upper limb. Averaging the data for all porphyroblasts containing inclusion trails that do not have the lower limb dip direction gives 3.29 mm. Thus the zones of progressive shortening strain that contain porphyroblasts with inclusion trails dipping in the opposite direction to those in the lower limb are 54.8%, on average, the width of those in the lower limb.

3.2. Millipede shaped inclusion trails in porphyroblasts

Fig. 9 shows the foliation relationships preserved in and around a porphyroblast from the hinge of the fold in Fig. 7, where S_2 in the matrix lies at a high angle to the sub-horizontal axial plane S_3, but where S_2 preserved as inclusion trails lies at a quite oblique angle. There is a spectacular increase in the separation of S_2 foliation planes as they exit into the matrix (shown in Figs. 9a,b) with the distance parallel to S_3

Table 1
Shows the pitch of S_2 preserved as inclusion trials in plagioclase porphyroblasts in the hinge plus lower and upper limbs of the fold shown in Fig. 8

Location	S_2 pitch SE in degrees	S_2 pitch NW in degrees
Upper limb	80	65
	82	80
	76	72
		75
		65
		72
Average	79.33	71.50
Hinge of fold	45	75
	89	88
	50	81
	77	80
	75	82
		75
Average	67.2	80.12
Lower limb	71	
	60	
	70	
	89	
	51	
	74	
Average	69.17	

The pitches were measured from the 12 thin sections taken from the fold profile plane shown in Fig. 8b. Note how only SE pitches are present in the lower limb.

Table 2
Shows the width between S_3 seams measured across porphyroblasts along the line W shown in Fig. 9a separated according to whether the S_2 inclusion trails dip SE or NW in 3-D plus whether the sections were cut from the hinge or lower and upper limbs of the blocks shown in Figs. 8b,c

Location	Width between S_3 for SE pitch in mm	Width between S_3 for NW pitch in mm
Upper limb	2.7	1.00
	7.7	4.00
	6.75	5.00
	2.45	8.45
	3.80	3.85
	3.25	3.55
	4.10	3.70
	9.25	2.40
		1.60
Average	5.00	3.73
Hinge of fold	4.25	3.85
	4.60	1.90
	4.45	2.30
	4.00	0.85
	4.25	2.30
	2.70	4.60
	1.90	
	8.60	
Average	4.34	2.63
Lower limb	0.60	
	9.25	
	8.30	
	4.15	
	6.90	
	3.10	
	10.35	
	5.40	
	4.60	
	7.30	
Average	6.00	

The dimension W defines the width of the zone of partitioned shortening strain that contains a porphyroblast.

increasing 1.83 times from inside to outside the porphyroblast. At high magnification, the matrix above and below the porphyroblast is dominated by a clockwise asymmetry of curvature of crenulated S_2 into sub-horizontal differentiated crenulation cleavage S_3 (Figs. 9d,e). This differentiation asymmetry is opposite to the anticlockwise shear required if the porphyroblast had been rotated to this orientation after or while it grew. However, in the strain shadow regions to the immediate left and right of the porphyroblast (Figs. 9 and 10) the differentiation asymmetry of S_2 into S_3 is anticlockwise (Figs. 10b,c), which is the shear sense required to rotate the S_2 foliation prior to it being overgrown by the porphyroblast. The pattern of S_1 and S_2 preserved within the strain shadows can be used to test this (Fig. 10). S_2 is a differentiated crenulation cleavage with an anticlockwise differentiation asymmetry due to the curvature of S_1 into S_2 (outside of the strain shadow in Fig. 10b). In Fig. 10b, the triangular shaped portion of S_2 in the strain shadow to the right of the porphyroblast is bounded by S_3 on its upper and lower margin with an anticlockwise differentiation asymmetry of S_2 into S_3. This differs from the clockwise differentiation asymmetry that dominates the matrix above and below. Within this triangular portion, as well as within the region now overgrown by the porphyroblast, if clockwise reactivation of S_2 occurred during D_3 rather than development of an S_3 axial plane cleavage (Bell, 1986), this would have resulted in the primary anticlockwise S_1/S_2 differentiation asymmetry being switched to clockwise and produce the geometry shown in Figs. 10a,b. Fig. 10c shows the rotational effect that such a process would have on S_2 within an ellipsoidal pod of partitioned strain prior to porphyroblast growth.

Figs. 10a,b shows that the crenulated cleavage S_1 can be seen between differentiated S_2 seams in the matrix but not in the porphyroblast in a profile plane section (Figs. 8a,b) cut perpendicular to L_3^2. This occurs for all 12-profile plane sections that we cut. All sections cut perpendicular to S_3 and parallel to L_3^2 (Figs. 8a,c) show crenulated S_1 in the porphyroblasts between differentiated S_2 seams but not in the matrix. Therefore, L_2^1 lies sub-parallel to L_3^2 in the matrix but sub-perpendicular to it in the porphyroblasts. Furthermore, L_3^2 changes from porphyroblasts to matrix in sections cut parallel to S_3 as shown in Fig. 8a.

3.2.1. Interpretation of trend of L_3^3

The above combination of facts allow us to derive the orientation of the stretching lineation L_3^3, within the axial plane structure S_3 even though we cannot observe it directly because of the seamy nature of S_3. The S_3 seams developed post porphyroblast growth. Therefore, L_2^1 was rotated during D_3 in the matrix but not in the porphyroblasts. Such rotation in more highly strained portions of rock always occurs towards the developing stretching lineation L_3^3 (e.g., Alsop and Holdsworth,

2004). Therefore, L_3^3 must trend at a low angle to the matrix intersection lineation L_3^2 as shown in Fig. 8a. A significant result of the low angle between L_3^2 and L_3^3 is that the displacement of S_2 across S_3 differentiated crenulation cleavage seams is minimalized in sections parallel to the profile plane (e.g., Figs. 9b–e), enhancing the coaxial nature of the resulting matrix geometry and possibly the millipedes.

3.3. Millipedes in 3D

Johnson and Moore (1996) used the computer program Mathematica® to produce a three-dimensional representation of a millipede porphyroblast microstructure from one of our samples of Robertson River Metamorphics, Australia collected from the same location as that shown in Figs. 5c–11. Foliations and porphyroblast outlines in a set of 12 closely spaced parallel thin sections were scanned and traced before being imported into Mathematica. The foliation surfaces and porphyroblasts were then reconstructed by redefining the traced curves as functions with a fitting algorithm. The 3D surfaces were then defined using a second set of functions using the techniques in Johnson and Moore (1993, 1996) and Moore and Johnson (1993, 2001). While the results obtained from Mathematica show the major features of the structure quite well, the fitting routines significantly simplify and smooth the final result. The scope for exploring the 3D nature of the structure in Mathematica is also extremely limited. We present a different version of the same millipede structure, reconstructed with the 3D modelling, animation and rendering package Discreet 3D Studio Max™.

The 12 traced sections (from Fig. 9 in Johnson and Moore, 1996) were digitized and imported into 3ds Max, where they were scaled and positioned using a vertical spacing of 1.5 mm (Fig. 12a). Once in position, the foliation and porphyroblast surfaces were reconstructed by stretching "U-loft" surfaces between the traced curves. This is akin to stretching a skin over a set of ribs and is demonstrated in Figs. 12b,c. These show the 12 curves that define one of the foliation surfaces (Fig. 12b) and the resulting surface created between the curves (Fig. 12c). The final model (Fig. 12d) is composed of the 5 individual foliation surfaces (light grey) and 3 plagioclase porphyroblasts (dark grey).

The geometry of foliation surfaces can be now examined and computer derived 2-D cuts made at any orientation. Horizontal and vertical slices through the model are presented in Figs. 13–15. The oppositely concave nature of the foliation surfaces is readily apparent in nearly all sections made through these models and reflect the structures observed in thin sections cut horizontally (Fig. 11) and vertically (Fig. 9) through sample H20C from the Robertson River Metamorphics. The millipede structures preserved in this sample can essentially be described as oppositely facing irregular cup shaped folds where they pass into the matrix and this is best seen by accessing the 3-D VRML model that can be accessed at http://www.es.jcu.edu.au/research/SAMRI/millipede.zip. Sections cut at almost any orientation (Fig. 15) will display

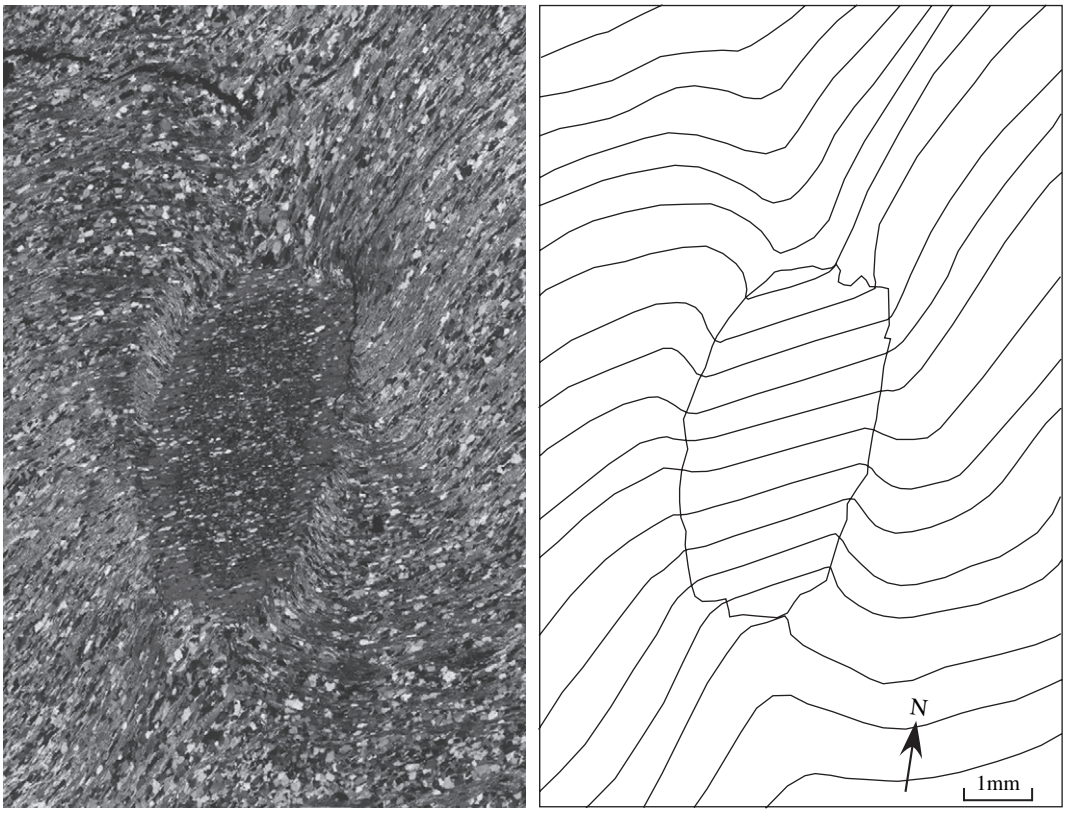

Fig. 11. Millipede plagioclase porphyroblast in a sub horizontal section cut parallel to the axial plane structure (S_3) of the F_3^2 fold that generated the millipede geometry. North is marked so that the structures preserved can be related to those in Fig. 8a. Crossed polars.

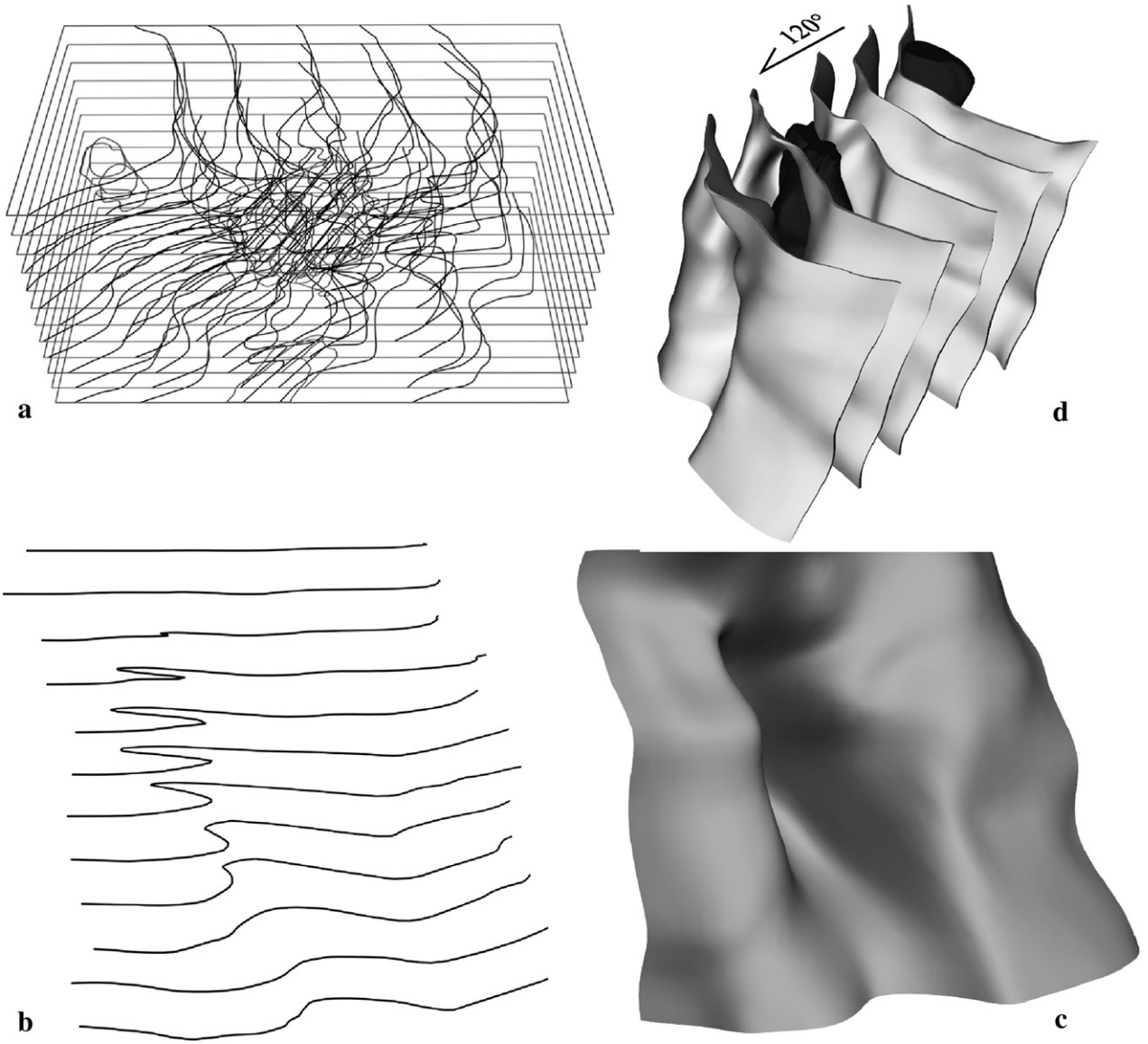

Fig. 12. Reconstruction of millipede structure after Johnson and Moore (1996). (a) Digitized and scaled tracings of 12 thin sections positioned with a spacing of 1.5 mm. (b) 12 curves define a single foliation surface. (c) ''U-loft'' surface created by stretching a skin over the curves. (d) Complete millipede model composed of five foliation surfaces (light grey) and three plagioclase porphyroblasts (dark grey). The single barbed arrow shows the strike and orientation of a face that is vertical when the sample is spatially oriented.

spectacular oppositely concave folds. The only sections that do not consistently display millipede shaped inclusion trail geometries are those cut sub-vertical and perpendicular to the fold profile plane.

4. Interpretation and discussion

4.1. Deformation history versus geometry

When first discovered, the millipede geometry appeared to provide a unique example of a structure that could only be produced by a history of progressive bulk inhomogeneous shortening (Bell and Rubenach, 1980). Recognition that a similar geometry could be produced experimentally during progressive inhomogeneous shearing (Figs. 4b,c) appeared to change this (Johnson and Bell, 1996). However, millipede-like shapes developed in the foliation being folded experimentally during bulk shear are only superficially similar to those that form in and around actual porphyroblasts (compare Figs. 5a–c). In examples of millipedes preserved by porphyroblasts, the matrix foliation follows the axial plane of the folds to either side of the central core structure. These are shown by the two lines of hinges marked with heavier black lines in Fig. 5c. The matrix ''foliation'' in the models produced experimentally by inhomogeneous simple shear does not follow the axial plane of the folds to either side of the central core structure. Instead, this foliation cuts across the millipede-like structure into the ''porphyroblast'' (Figs. 5a,b). This simple test is readily applied to naturally occurring millipedes allowing them to be used to distinguish the deformation history. This is a significant

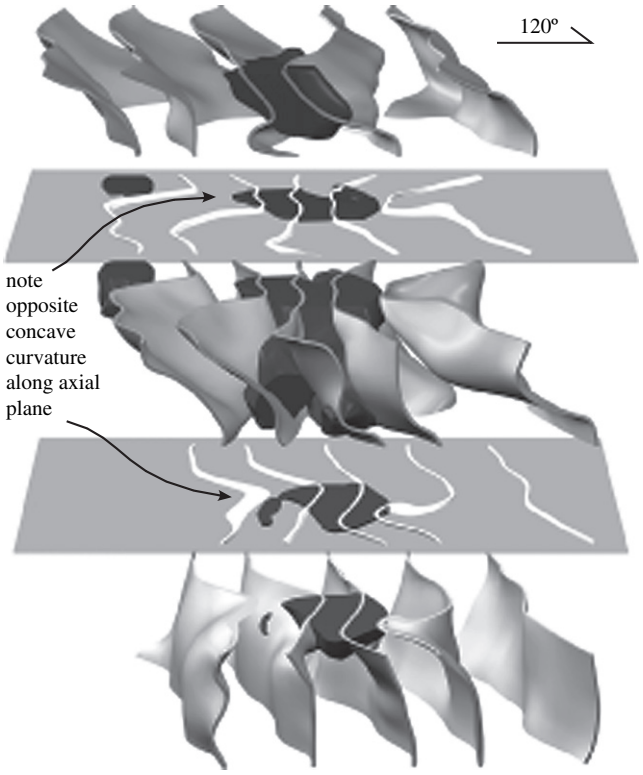

Fig. 13. Two horizontal slices cut through the millipede model displaying oppositely concave foliation traces. The single barbed arrow shows the strike of the vertical face on the front of the structure.

breakthrough because millipede geometries around porphyroblasts are found relatively commonly when vertical thin sections are cut around the compass rather than oriented relative to the matrix foliation.

4.2. The progressive development of the fold

To understand how this fold developed (Fig. 16) we have to be able to explain why the straight portion of S_2 inclusion trails, which dominate all porphyroblasts, pitch only SE on the lower limb of the fold (Figs. 7 and 8), but both SE and NW in the hinge and upper limb (Table 1). We also have to be able to explain why all porphyroblasts, independent of whether their S_2 inclusion trails pitch SE or NW, contain millipede inclusion trail geometries on their rims that developed during the same deformation that produced the fold.

The curvature of crenulated S_2 into differentiated S_3 (called the S_3 differentiation asymmetry) is dominantly clockwise in the matrix away from the porphyroblasts on both limbs of the fold. Therefore, shear on S_3, once differentiation became significant, was predominantly clockwise, or top to the SE in Figs. 7 and 8 (shown schematically in Figs. 6d–f) and could rotate S_2 from SE pitches to NE pitches but not vice versa (Figs. 16a–c). However, the millipede geometries trapped within the porphyroblasts reveal that they all grew during coaxial bulk shortening. Consequently, those with SE pitching S_2 inclusion trails on the hinge and upper limb probably grew before the fold developed as shown in Fig. 16d. Those with NW pitching S_2 inclusion trails in the hinge and upper limb porphyroblasts (Fig. 16f) would have grown after the upper NW dipping limb began to form (Fig. 16e) when these portions of the fold contained NW pitching S_2 and the lower limb did not. This interpretation of the history of fold development is supported by the change in width of the zones of progressive shortening shown in Table 2, which for NW pitches decreases to 54.8% the width of the zones with SE pitches in the lower limb, suggesting that progressive shearing repartitioned at

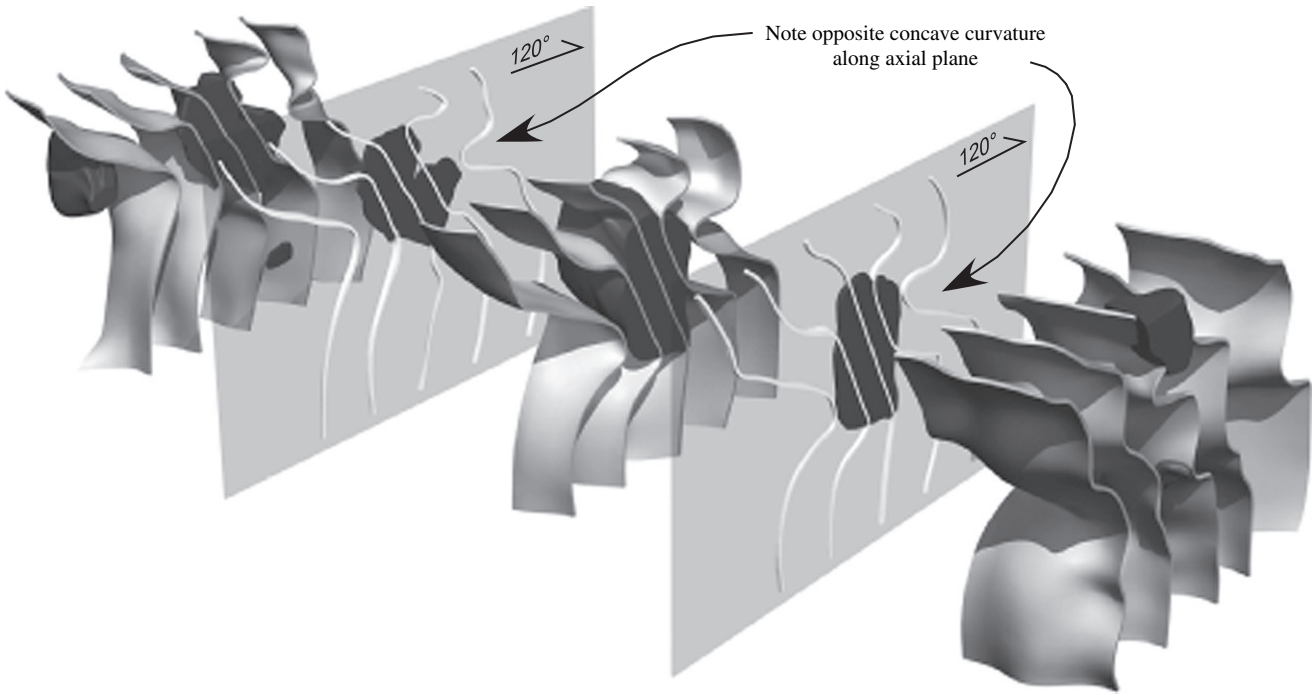

Fig. 14. Vertical millipede sections displaying oppositely concave foliation traces. The single barbed arrows show the strike of vertical cuts through the structure.

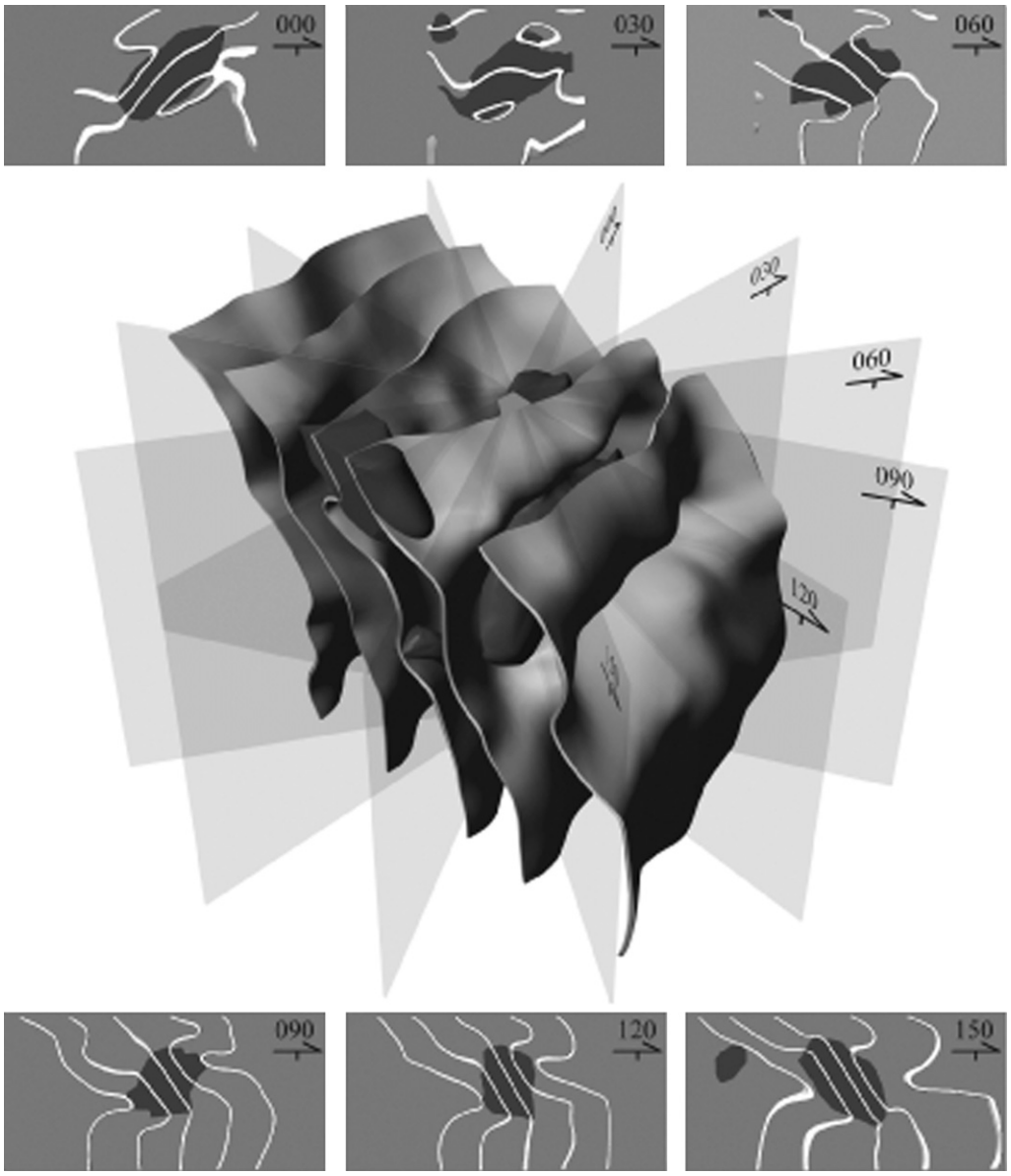

Fig. 15. Radial sections through the millipede model display spectacular oppositely curving foliation traces in sections of almost any orientation. The single barbed arrows shows the strike of successive vertical cuts.

a finer scale in these regions to develop the upper limb of the fold as shown in Fig. 16f.

We interpret that the fold formed by progressive bulk inhomogeneous shortening with a component of top to the SE shear (e.g. Bell and Hickey, 1997; Ham and Bell, 2004). However, if only clockwise shear occurred on developing S_3, an enormous amount of bulk shortening would have been required to rotate S_2 in the lower limb to its lowest local pitch of 20°. This is shown in Fig. 16 where 100% homogeneous bulk shortening of Fig. 16b produced SE pitches only as low as 45° in Fig. 16c. This suggests there was some local top to the NW or anticlockwise shear on the lower limb. Detailed examination of the location where the lower limb locally pitches 20°SE revealed that an anticlockwise differentiation asymmetry on S_3 is very locally present.

Of course local components of clockwise and anticlockwise shear (Figs. 2a,b) must have been present to form the millipede geometries; rotation of S_2 occurred in opposite directions along the same S_3 axial plane during the early stages of D_3 (e.g., Figs. 6a–c) as can be seen in Figs. 9a,b. Therefore, during porphyroblast growth (e.g. Figs. 6a–c) no pattern of non-coaxiality had developed and crenulations with both asymmetries developed. However, the final dominance in the matrix of a clockwise differentiation asymmetry for S_3 across the fold suggests that from the commencement of progressive bulk inhomogeneous shortening during D_3, although the deformation was essentially coaxial, there was a small component of top to the SE displacement. This rotated S_2 into steeper orientations until it dipped NW and started to form alternate folds limbs (e.g. Fig. 16e). This

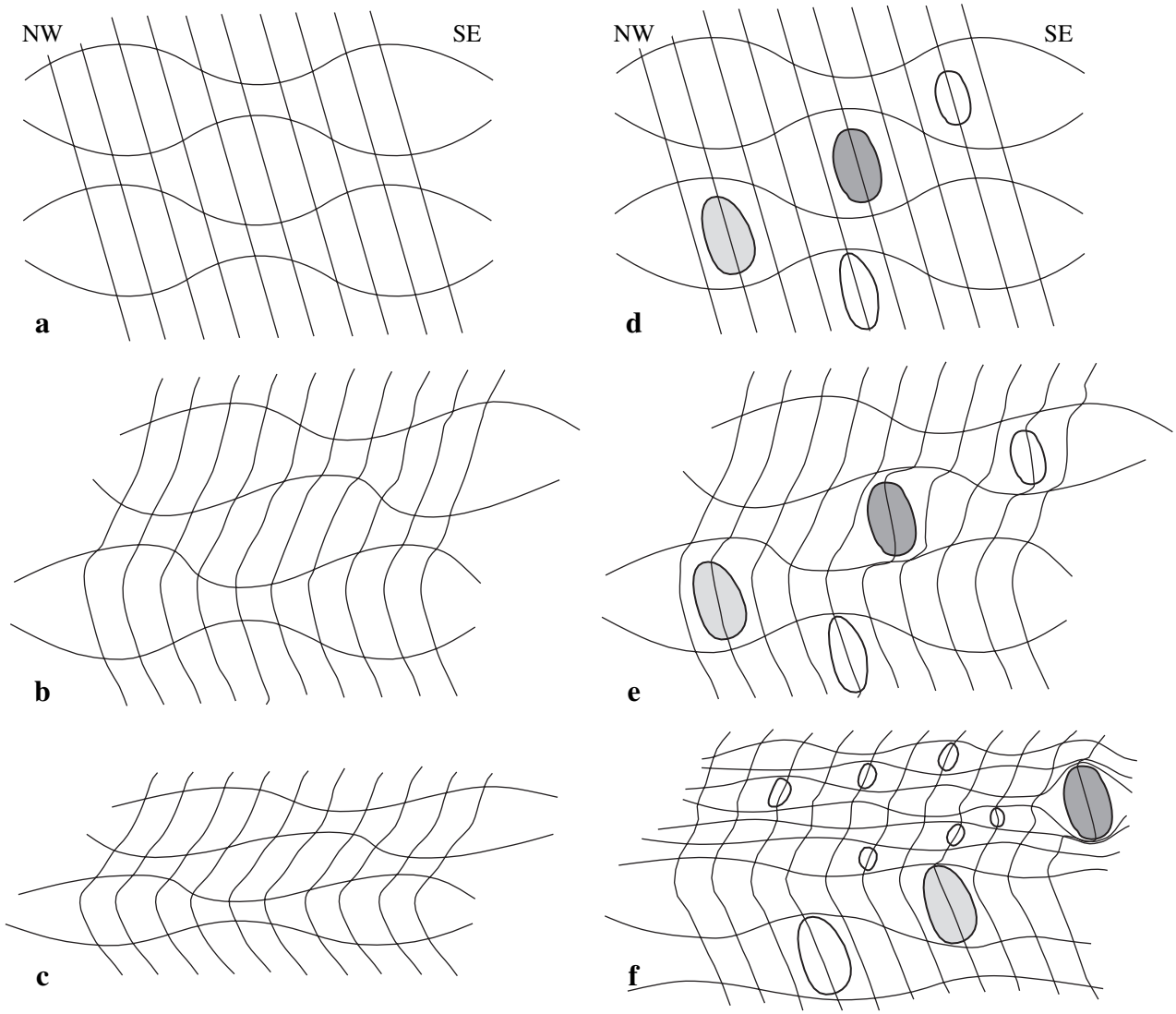

Fig. 16. Sketches showing how bulk shortening of an initially 70°SE dipping S_2 foliation (a) and only clockwise shear on the sub-horizontal axial plane differentiated crenulation cleavage S_3 (b) cannot produce the lowest angles (locally as low as 20° to the horizontal) of limb dip on lower limb (c) seen in the fold in Fig. 7. Therefore, early during the deformation history there must have been some anticlockwise shear on the lower limb. (d) porphyroblast growth early in the history of bulk shortening preserves inclusion trails with the initial orientation after folding has commenced. (e, f) Shows the effects of a reduction in the scale of partitioning on the upper limb of a fold as the deformation intensified. Newly grown porphyroblasts in the progressive shortening domains after repartitioning occurred have smaller dimensions perpendicular to the axial plane.

explains the preservation of porphyroblasts with inclusion trails pitching SE on both limbs in profile plane thin sections (Fig. 16d). Those porphyroblasts in the hinge and on the upper fold limb containing inclusion trails that vary through the vertical to pitching steeply NW lie in domains wrapped by S_3 that are 54.8% on average shorter in width than those containing porphyroblasts in the lower limb where all the inclusion trails pitch SE (Fig. 16f). This suggests that the deformation during D_3 repartitioned at a smaller scale in the zones that became hinges and NW dipping limbs (compare Figs. 16e,f) in this outcrop. This repartitioning resulted in the nucleation and growth of more porphyroblasts that have smaller widths perpendicular to S_3, but which preserve millipede shaped inclusion trails because the deformation was still dominantly coaxial.

4.3. The progressive development of deformation partitioning

Large-scale orogenesis can be a response to crustal shortening, or gravitational collapse of an over thickened orogen; collapse can result from over thickening due to excessive crustal shortening or from extension due to roll back (e.g., fig. 14 in Bell and Newman, 2006). Such large-scale modes of deformation occur by a general history of progressive bulk inhomogeneous shortening at a low angle to σ_1. Within the orogen, the deformation partitions into portions where a large component of progressive bulk shortening accompanies and even results in the development of significant zones of progressive shearing such as mylonite zones on major thrusts (e.g., fig. 18 in Bell and Newman, 2006). Zones of progressive inhomogeneous

shear (i.e., where there is no component of bulk shortening across the shear zone) tend to be restricted to vertical transform or transfer faults where, geometrically, there is no role for bulk shortening. Determining the progressive development of deformation partitioning has generally been an unresolved problem in orogenic belts because the deformation repartitions through the rocks at finer and finer scales as it intensifies. Porphyroblasts provide the best evidence for the role of partitioning in deformation history because they preserve the microstructures that they overgrow from obliteration as the deformation intensifies. Indeed, they provide the only source of data on what took place geometrically in a rock prior to the intensification of the matrix foliation. Porphyroblasts always nucleate and grow prior to the commencement of differentiated crenulation cleavage development (e.g., Spiess and Bell, 1996; Fig. 1 in Bell et al., 2004). Consequently, for any deformation event that was very intense, they preserve evidence of the character of the deformation partitioning at the initial stages of impact of that event on the rock (e.g., Figs. 6a–c); they cease to grow once the deformation intensifies to such a level that a differentiated crenulation cleavage begins to form in their immediate vicinity (Figs. 6d–f; Bell et al., 2004).

4.3.1. Reactivation weakening in fold hinges

The fold hinge in Fig. 7a preserves other intriguing information on the role of deformation partitioning in these rocks during the early stages of deformation. Sub-horizontal S_3, which accompanied the development of this fold, is dominated by a clockwise differentiation asymmetry on both limbs and the hinge (Figs. 9d,e). This indicates that top to the SE shear accompanied bulk shortening as this foliation and the fold developed (Bell and Johnson, 1992). Of course the opposite (anticlockwise) asymmetry is preserved in the rims of all porphyroblasts and in the strain shadows of some (e.g., Fig. 10b), as millipede geometries could not develop without both shear senses occurring at the same time (e.g., Figs. 2a,b). Furthermore, in one location where the limb pitch in the profile plane on the lower limb locally reduces to 20°, an anticlockwise differentiation asymmetry is very locally preserved away from porphyroblasts.

S_2 preserved as inclusion trails in porphyroblasts on the lower limb always pitches in the one direction averaging around 70° to the SE (Table 1). Similarly pitching S_2 trails in the hinge and upper limb, as well as others that pitch NW (Table 1), plus the dominant top to the south SE shear on S_3, suggest that S_2 dipped 70° to the SE in the early stages of D_3 as shown in Fig. 16d and discussed earlier. However, due to the effects of early reversals in shear that predated the final all pervasive clockwise shear that dominates the matrix, S_2 was locally rotated anticlockwise as shown in Figs. 9 and 10. This rotation took place without the pervasive development of a differentiated S_3 by antithetic shear on S_2 (Fig. 10c) after it had rotated sufficiently from a high angle to the newly developing D_3 axial plane to be reactivated (Bell, 1986). Furthermore, the amount of anticlockwise rotation of S_2 was large (Figs. 9 and 10); this is particularly significant because this rotation occurred in a local and isolated ellipsoidal zone (Fig. 10c) within the fold hinge where S_3 was developing near orthogonal to S_2 (Figs. 9a–c). This extraordinary setting for such an anomalous amount of rotation of the foliation being folded strongly suggests that the interaction of synthetic shear on a newly developing axial plane structure and antithetic shear on a well developed foliation that is being folded can have runaway effects in terms of the amount of strain that can be locally accumulated over a short period of the deformation history. It suggests that if the circumstances are right, after some critical amount of rotation, such a geometry can literally collapse like a pack of cards as shown in Fig. 10c, but by a completely ductile process. The critical amount of rotation of a pre-existing foliation away from orthogonal to the newly developing one lies somewhere between 20° and 40°.

4.3.2. Reactivation weakening – a mechanism for crenulation cleavage development and switching off porphyroblast growth

The anomalous rotation of S_2 prior to porphyroblast growth (Fig. 10) in the hinge of the fold in Fig. 7 has implications for the mechanism of differentiated crenulation cleavage development and the switching off of porphyroblast growth that takes place as differentiation begins (e.g., Bell et al., 2004). Crenulation cleavage development during the 1960's and 1970's was considered to be a product of buckling and dissolution of the long limb through a mechanism of pressure solution involving the effect of stress differentials on chemical potential (e.g., Gray and Durney, 1979). However, stress differentials around a grain do not accumulate as the deformation continues; they vary as deformation occurs and remain small making it difficult to accept them as a significant driving force for the slow process of dissolution and solution transfer.

An alternative mechanism was proposed in the 1980's involving the effects of deformation partitioning. This mechanism suggests differentiated crenulation cleavage seams form along zones of progressive shearing (e.g., Fig. 1; Bell, 1981). When a zone of progressive shearing begins to form, dislocation densities accumulate in non-platy minerals within this zone; this increases chemical potential gradients from the rim to core causing dissolution and removal of the rim and eventually of the whole. This brings together platy minerals, which do not accumulate dislocations, into differentiated crenulation cleavage seams (Figs. 6d–f; Bell and Cuff, 1989). After initiation of the zone of progressive shearing, non-platy minerals on the margins of these zones are progressively strained increasing chemical potential gradients from rim to core these grains and causing their dissolution and removal. The platy (and locally some fibrous) minerals are left behind as cleavage seams that widen the more shear strain that has occurred along the zone of progressive shearing (Bell and Cuff, 1989). In this model, bulk shear operates along the crenulation cleavage seam, as shown in Figs. 1 and 6d,e, and equates with that acting along S_3 in Figs. 7–9.

In the early stages of crenulation development, once some rotation of the crenulated cleavage has occurred, reactivational shear along this cleavage (S_2 in the case described herein) can occur. If rapid collapse of this zone occurred, similar to that

discussed in the previous section, then differentiated cleavage development may occur through the same reactivational weakening process. This could go a long way to help explaining the link between the cessation of porphyroblast growth and the commencement of this stage of crenulation cleavage development that has been observed and pondered over for 2 decades (e.g., Spiess and Bell, 1996).

4.4. Millipedes in 3D

Figs. 13–15 show that millipede geometries can be seen in most thin section orientations within porphyroblasts. This is not the case for cut effect millipede-like geometries that are common in thin sections cut sub-parallel to foliation intersection/inflection axes preserved in porphyroblasts (FIAs) containing spiral shaped inclusion trails. As shown in Figs. 13–15, where the inclusion trails are continuous with the matrix foliation, millipede geometries can be seen in almost all thin sections orientations. The only orientation where they tend be uncommon is for thin sections cut parallel to the L_3^2 and perpendicular to S_3 such as the 030° section in Fig. 15. This has considerable significance because even where porphyroblasts pre-date the matrix foliation and are completely truncated by it, millipede geometries will be preserved in most thin section orientations within the porphyroblasts and revealed in spite of cutting sections relative to the matrix microstructures. Therefore, if two or more differently oriented sections are cut relative to geographic coordinates, and the porphyroblasts contain millipede microstructures, these will be revealed in at least one of these sections. For the discerning reader we have constructed a virtual reality model (VRML), which can be accessed on the world wide web at the URL http://www.es.jcu.edu.au/research/SAMRI/millipede.zip. This model allows the reader to examine the millipede geometry in Figs. 13–15 in full colour in 3-D and rotate it for observation from any direction. At the push of a button the model will split along the planes shown in Fig. 14.

4.5. Cut effect millipede-like structures

Stallard et al. (2002) make the assertion that millipede microstructures may simply represent a peculiar 2-D slice

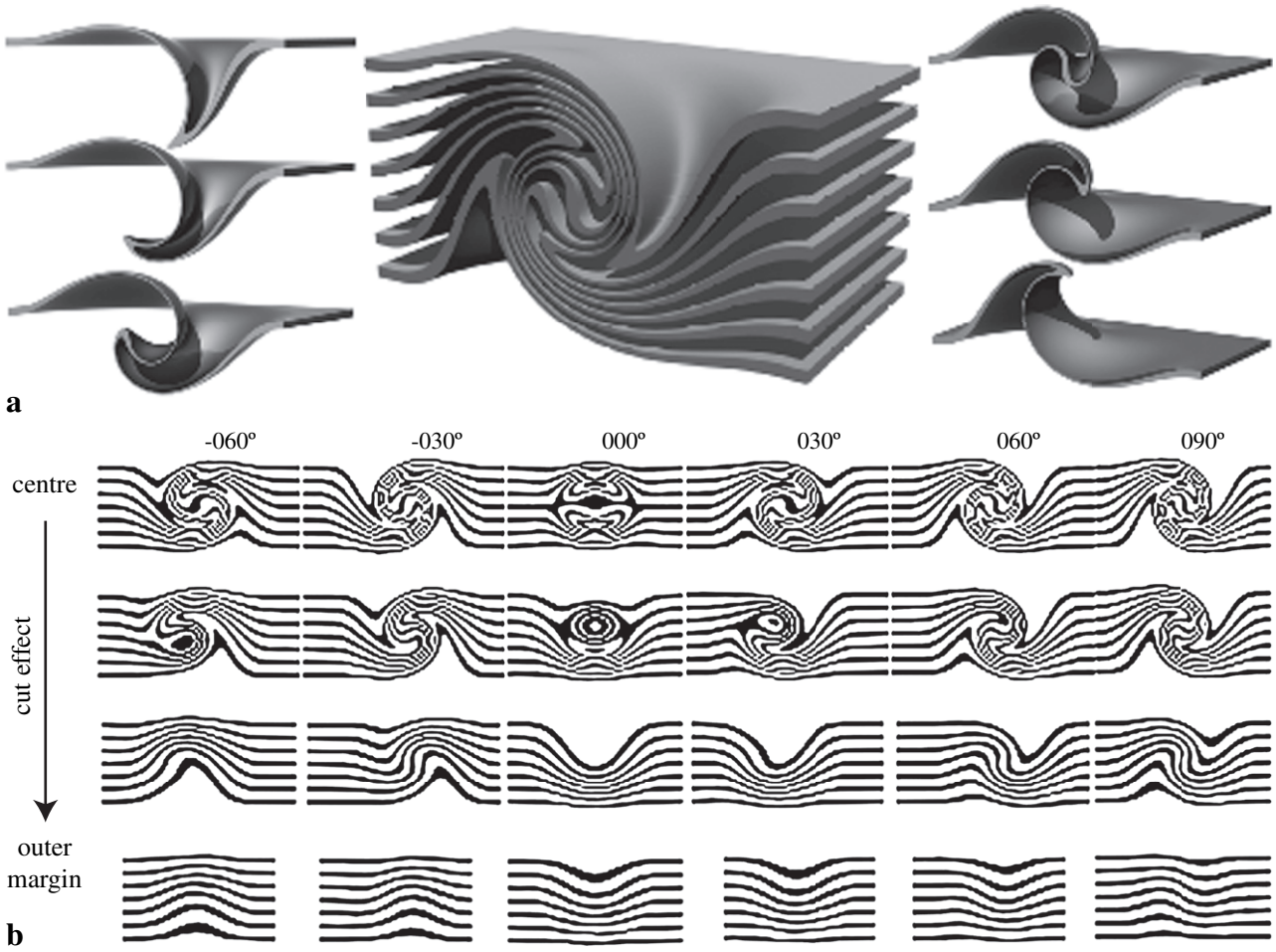

Fig. 17. (a) Cut-away profile view of a model spiral structure with the elements of this model separated to either side (*c.f.* Stallard et al., 2002). (b). Shows the range of inclusion trail geometries expected in a series of radial thin sections through a sample containing spiral porphyroblasts. Sections in the top row pass through the centre of the model; those in the bottom row intersect the outer edge. Orientations are given relative to the axis of apparent rotation. Only sections cut parallel to the axis of rotation display foliation traces that could be mistaken for millipede structures, all others show spirals or sigmoids.

through a 3-D spiral. Certainly, as mentioned above, cut effect millipede-like structures appear when thin sections are cut parallel to the FIA through natural spiral inclusion trails preserved in porphyroblasts. We compared several computer-derived slices through a simple model spiral, constructed using the ''soft selection'' tool in 3D Studio Max with slices through an actual millipede. A rotation of 270° was applied to the central vertex of a model composed of seven parallel sheets, each defined by 100 × 100 × 5 vertices. The effect produced was that the central part of the model was rotated 270° with a decreasing amount of rotation with distance away from the central vertex. A cut-away view of the model spiral is shown in Fig. 17a. The separated elements of the spiral in Fig. 17a compare favourably with those produced by Stallard et al. (2002). Sections cut parallel to the axis of rotation show oppositely curved or closed-loop structures (000° in Fig. 17b). These structures may exhibit a resemblance to sections through genuine millipedes. However, the opposite extremities of the curving inclusion trails tend to start to bend back towards each other, in some cases making a closed loop (compare Figs. 17b and 15), in complete contrast with true millipedes, which never have this character. We have also shown that sections of almost any orientation through genuine millipede structures will display oppositely curving foliation traces. The converse is true for sections through spirals. Only sections cut very close to the axis of rotation will display such structures. The vast majority of sections will display either spirals or simple sigmoidal foliation traces (Fig. 17b). Therefore, it is relatively easy to distinguish cut effect millipede-like structures from true millipedes. One simply needs to cut a thin section striking at 45° to the one in which the millipede-like geometry appeared. If spiral inclusion trails are revealed, then the geometry was produced by a cut effect.

4.6. Transection of sheath fold hinges

Alsop and Holdsworth (2004, p. 1578) described natural sheath folds where the intersection lineation of the foliation being generated transects the hinge line. Alsop and Holdsworth (unpublished data) have been exploring ways of discriminating zones of high strain containing sheath folds resulting from a deformation history of inhomogeneous simple shear from those that formed during bulk inhomogeneous shortening. If transection occurs in samples where the deformation history was of the former type (Alsop, G.I. pers. comm. 2006), but not in those where it was the latter, this would be of considerable interest. It might reflect the transection of fold axial plane geometries resulting from the inhomogeneous simple shear experiments discussed herein and eventually provide a quantifiable discriminator of deformation history for sheath fold development. One would have to be certain that the sheath folds formed at the same time as the cleavage rather than being overprinted by it because it is now apparent that the latter history is common in regional folds (Ham and Bell, 2004; Bell et al., 2005).

5. Conclusions

Millipede structures with an axial plane foliation can only form by progressive bulk inhomogeneous shortening.

Millipede-like shapes transected by a foliation that accompanied their development form during progressive inhomogeneous simple shear.

Acknowledgements

We acknowledge the ARC for providing the funding that enabled this research to be conducted. We also acknowledge the constructive input from 4 referees on 2 earlier versions of this manuscript.

References

Aerden, D.G.A.M., 1991. Foliation-boudinage control on the formation of the Rosebery Pb-Zn orebody, Tasmania. Journal of Structural Geology 13, 759–775.

Alsop, G.I., Holdsworth, R.E., 2004. The geometry and topology of natural sheath folds: a new tool for structural analysis. Journal of Structural Geology 26, 1561–1589.

Beaumont-Smith, C.J., 2001. The role of conjugate crenulation cleavage in the development of 'millipede' microstructures. Journal of Structural Geology 23, 973–978.

Bell, T.H., 1981. Foliation development: the contribution, geometry and significance of progressive bulk inhomogeneous shortening. Tectonophysics 75, 273–296.

Bell, T.H., 1986. Foliation development and refraction in metamorphic rocks: reactivation of earlier foliations and decrenulation due to shifting patterns of deformation partitioning. Journal of Metamorphic Geology 4, 421–444.

Bell, T.H., Cuff, C., 1989. Dissolution, solution transfer, diffusion versus fluid flow and volume loss during deformation/metamorphism. Journal of Metamorphic Geology 7, 425–448.

Bell, T.H., Hickey, K.A., 1997. Distribution of pre-folding linear movement indicators around the Spring Hill Synform, Vermont: significance for mechanism of folding in this portion of the Appalachians. Tectonophysics 274, 275–294.

Bell, T.H., Johnson, S.E., 1989. The role of deformation partitioning in the deformation and recrystallization of plagioclase, orthoclase and microcline in the Woodroffe Thrust Mylonite Zone. Journal of Metamorphic Geology 7, 151–168.

Bell, T.H., Johnson, S.E., 1992. Shear sense: a new approach that resolves problems between criteria in metamorphic rocks. Journal of Metamorphic Geology 10, 99–124.

Bell, T.H., Newman, R., 2006. Appalachian orogenesis: the role of repeated gravitational collapse. In: Butler, R., Mazzoli, S. (Eds.), Styles of Continental Compression. Special Papers of the Geological Society of America 414, 95–118.

Bell, T.H., Rubenach, M.J., 1980. Crenulation cleavage development – evidence for progressive bulk inhomogeneous shortening from ''millipede'' microstructures in the Robertson River Metamorphics. Tectonophysics 68, T9–T15.

Bell, T.H., Ham, A.P., Hickey, K.A., 2003. Early formed regional antiforms and synforms that fold younger matrix schistosities: their effect on sites of mineral growth. Tectonophysics 367, 253–278.

Bell, T.H., Ham, A.P., Kim, H.S., 2004. Partitioning of deformation along an orogen and its effects on porphyroblast growth during orogenesis. Journal of Structural Geology 26, 825–845.

Bell, T.H., Ham, A.P., Hayward, N., Hickey, K.A., 2005. On the development of gneiss domes. Australian Journal of Earth Sciences 52, 183–204.

Cihan, M., Parsons, A., 2005. The use of porphyroblasts to resolve the history of macro-scale structures: an example from the Robertson River

Metamorphics, North-Eastern Australia. Journal of Structural Geology 27, 1027–1045.

Davis, B.K., 1995. Regional-scale foliation reactivation and reuse during formation of a macroscopic fold in the Robertson River metamorphics, North Queensland, Australia. Tectonophysics 242, 293–311.

Davis, T.P., 2004. Mine-scale structural controls on the Mount Isa Zn-Pb-Ag and Cu orebodies. Economic Geology 99, 543–559.

Ghosh, S.K., 1975. Distortion of planar structures around rigid spherical bodies. Tectonophysics 28, 185–208.

Gray, D.R., Durney, D.W., 1979. Crenulation cleavage differentiation – implications of solution-deposition processes. Journal of Structural Geology 1, 73–80.

Ham, A.P., Bell, T.H., 2004. Recycling of foliations during folding. Journal of Structural Geology 26, 1989–2009.

Hayward, N., 1992. Microstructural analysis of the classic snowball garnets of southeast Vermont. Evidence for non-rotation. Journal of Metamorphic Geology 10, 567–587.

Johnson, S.E., Bell, T.H., 1996. How useful are ''millipede'' and other similar porphyroblast microstructures for determining syn-metamorphic deformation histories. Journal of Metamorphic Geology 14, 15–28.

Johnson, S.E., Moore, R.R., 1993. Surface reconstruction from parallel serial sections using the program Mathematica: example and source code. Computers and Geosciences 19, 1023–1032.

Johnson, S.E., Moore, R.R., 1996. De-bugging the 'millipede' porphyroblast microstructure: a serial thin-section study and 3-D computer animation. Journal of Metamorphic Geology 14, 3–14.

Lagoeiro, L., Hippertt, J., Lana, C., 2003. Deformation partitioning during folding and transposition of quartz layers. Tectonophysics 361, 171–186.

Moore, R.R., Johnson, S.E., 1993. Reconstruction of inclusion surfaces within metamorphic garnet crystals. Mathematica Journal 3, 70–75.

Moore, R.R., Johnson, S.E., 2001. Three dimensional reconstruction and analysis of complexly folded surfaces using Mathematica. Computers and Geosciences 27, 401–418.

Sayab, M., 2005. N-S shortening during orogenesis within the Mt Isa Inlier (NW Queensland, Australia): the preservation of early W-E trending foliations in porphyroblasts revealed by independent 3D measurement techniques. Journal of Structural Geology 27, 1445–1468.

Siame, L.L., Bellier, O., Sebrier, M., Araujo, M., 2005. Deformation partitioning in flat subduction setting: case of the Andean foreland of western Argentina (28 degrees S-33 degrees S). Tectonics 24, TC5003.

Spiess, R., Bell, T.H., 1996. Microstructural controls on sites of metamorphic reaction: a case study of the inter-relationship between deformation and metamorphism. European Journal of Mineralogy 8, 165–186.

Stallard, A., Ikei, H., Masuda, T., 2002. Quicktime movies of 3D spiral inclusion trail development. In: Bobyarchick, A., (Ed.). Visualisation, Teaching and Learning in Structural Geology. Journal of the Virtual Explorer 9, 17–30.

Stewart, L.K., 1997. Crenulation cleavage development by partitioning of deformation into zones of progressive shearing (combined shearing, shortening and volume loss) and progressive shortening (no volume loss): quantification of solution shortening and intermicrolithon-movement. Tectonophysics 281, 125–140.